

Electrochemical and Thermodynamic Estimations of the Interaction Parameters for Bulk and Nano-Silver Nitrate (NSN) with Cefdinir Drug Using a Glassy Carbon Electrode

S. E. El-Shereafy¹, E. A. Gomaa², A. M. Yousif¹ and A. S. Abou El-Yazed¹

* eahgomaa66@yahoo.com

Received: May 2017

Accepted: November 2017

¹ Chemistry Department, Faculty of Science, Minoufiya University, Shebin El Kom, Egypt.

² Chemistry Department, Faculty of Science, Mansoura University, Mansoura, Egypt.

DOI: 10.22068/ijmse.14.4.48

Abstract: The redox behavior for bulk and nano silver nitrate (NSN) were studied by cyclic voltammetry technique in absence and presence of cefdinir antibiotic (CFD) using glassy carbon electrode (GCE) in 0.1 M KNO₃ as supporting electrolyte at two different temperatures. Scan rates were studied for the redox reactions of bulk and nano silver nitrate (NSN) in absence and presence of cefdinir antibiotic (CFD) and mechanism of the electrode reactions were discussed. The stability constant of complexation and thermodynamic parameters for a system were evaluated.

Keywords: Cyclic Voltammetry, Thermodynamics, Cefdinir Antibiotic, Redox Reactions, Stability Constant.

1. INTRODUCTION

Silver nanoparticles were viewed as being moderately simple to synthesize [1,2] and having exceptionally attractive properties [3] or being helpful for particular applications such as electrochemical nitrate sensors [4,5], solar cells [6] or temperatures switches [7] and biology. Silver exists in two isotopic forms, ¹⁰⁷Ag and ¹⁰⁹Ag, found in similar proportions. Silver is present in the human body at very low concentrations (<2.3 μg l⁻¹) and is absorbed through the lungs, gastrointestinal tract, mucus membranes. It is retained for the most part as silver protein complexes but has no physiological or biochemical role within the body [8]. Silver is used in heterogeneous oxidation processes and homogeneous silver-mediated and catalysed reactions. Silver (I) is considered a mild oxidizing agent and, as is suitable for the efficient oxidation of primary and secondary alcohols to aldehydes and ketones [9]. Silver (I) was used as a catalyst in organic synthesis [10,11]. The research for silver (I) complexes with N-donor ligands, including those of aromatic ligands such as azoles [12,13] and O-donor ligands for complexation with silver (I) include carboxylates, crown ethers and calixarenes. Cefdinir (CFD) is a bacteriocidal antibiotic of

third-generation cephalosporin class of antibiotics. It can be used to treat infections caused by several Gram-negative and Gram-positive bacteria. its structural formula is shown in Fig. 1.

In the present work, we are interested in investigating the electrochemical behavior of the complexation of bulk AgNO₃ and nano-AgNO₃ (NSN) with cefdinir antibiotic (CFD) and from which we determined the stability constant of complex formed and estimated thermodynamic parameters for a system. Hence, the cyclic voltammetric behavior of cefdinir drug at a glassy carbon electrode and its complexation with bulk and nano-AgNO₃ (NSN) was studied in 0.1 M of KNO₃ as a supporting electrolyte in 5% mixed solvent (DMF-H₂O) at different temperatures (298.15, 303.15 K).

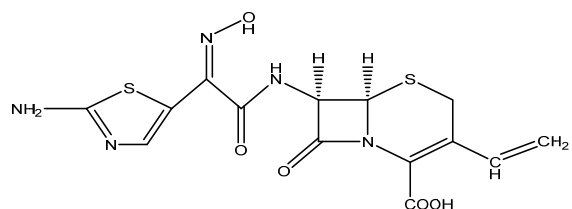


Fig.1. structural formula of cefdinir antibiotic.

2. EXPERIMENTAL

2. 1. Materials

Cefdinir antibiotic were purchased from sigma Aldrich and analyzed by utilizing transmission electron microscopy (TEM) and Infra-red (IR), silver nitrate (AgNO_3) from Merck Germany , dimethylformamide form El Nasr pharmaceutical chemicals Co. and used directly without purification, double distilled water was used throughout this study.

2. 2. Preparation of Nano-Silver Nitrate

The nano- silver nitrate (NSN) was prepared by shaking it in ball-mill apparatus of type Retsch MM2000 swing mill for period of one hour. The mill has 10 cm^3 stainless steel tube. Two stain steel balls of 12 mm diameter were used. Ball milling was performed at 20225 Hz at room temperature and investigated under transmission electron microscopy (TEM).

2. 3. Measurements

The glassy carbon electrode was polished to a mirror like surface with 0.5 and $0.02 \mu\text{m}$ alumina in doubly distilled water. experimental solution was deaired by purging for at least 10 minutes with 99.99% pure nitrogen gas. Three electrodes system consists of a GCE as the working electrode, Ag/AgCl (satd. KCl) as the reference electrode and platinum wire as the counter electrode was used. Cyclic voltammetric measurement was performed using a potentiostat Model BASi EPSILON.

3. RESULTS AND DISCUSSION

3. 1. TEM Image for Nano-Silver Nitrate

The picture of Nano- AgNO_3 from transmission electron microscope (TEM) is represented in Fig. 2 from an image we can deduce that nano- AgNO_3 (NSN) is either in the form of irregular or distorted spheres and the dimensions of the particles ranging from 11.40 to 26.91 nm.

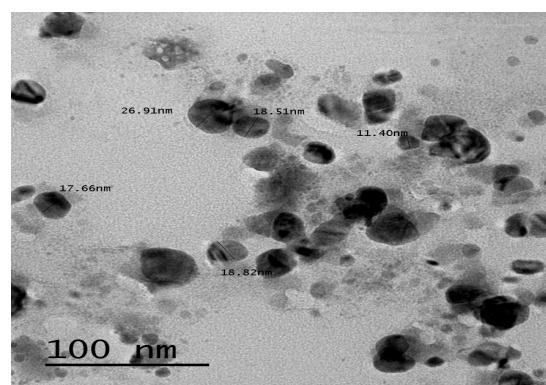


Fig. 2. TEM image of Nano- AgNO_3

3. 2. Electrochemical Behavior of Bulk AgNO_3 and Nano- AgNO_3 in Absence of Ligand (Cefdinir Antibiotic)

The redox behavior of Ag (I) in bulk AgNO_3 and nano- AgNO_3 (NSN) was examined in 0.1 M of KNO_3 as a supporting electrolyte in 5% mixed solvent ($\text{DMF-H}_2\text{O}$) by cyclic voltammetry on GCE at different temperatures (298.15, 303.15 K). This process is preformed at -600 to 650 mV potential window, current is (1mA) and 100 mV/S scan rate. in which silver nitrate solution is added in a stepwise manner to reach the final concentration is (1.9 mM) is shown in Fig. 3.

From (Fig. 3) it is observed that Ag^+ solution is electroactive as it gives one anodic and one cathodic peak (Ag^+/Ag). Firstly, (at 298.15 K) for bulk AgNO_3 anodic peak current is -0.392 mA and potential 509.3 mV. cathodic peak current is 0.154 mA and potential 270 mV for nano- AgNO_3 (NSN) anodic peak current is -0.186 mA and potential 476.2 mV. cathodic peak current is 0.0799 mA and potential 252.6 mV. Secondly, (at 303.15 K) for bulk AgNO_3 anodic peak current is -0.462 mA and potential 532.2 mV. cathodic peak current is 0.1844 mA and potential 227.9 mV. For nano silver nitrate (NSN) anodic peak current is -0.302 mA and potential 484.4 mV. cathodic peak current is 0.1228 mA and potential 252.6 mV. This indicates that the Ag^+ system is one electron reversible system.

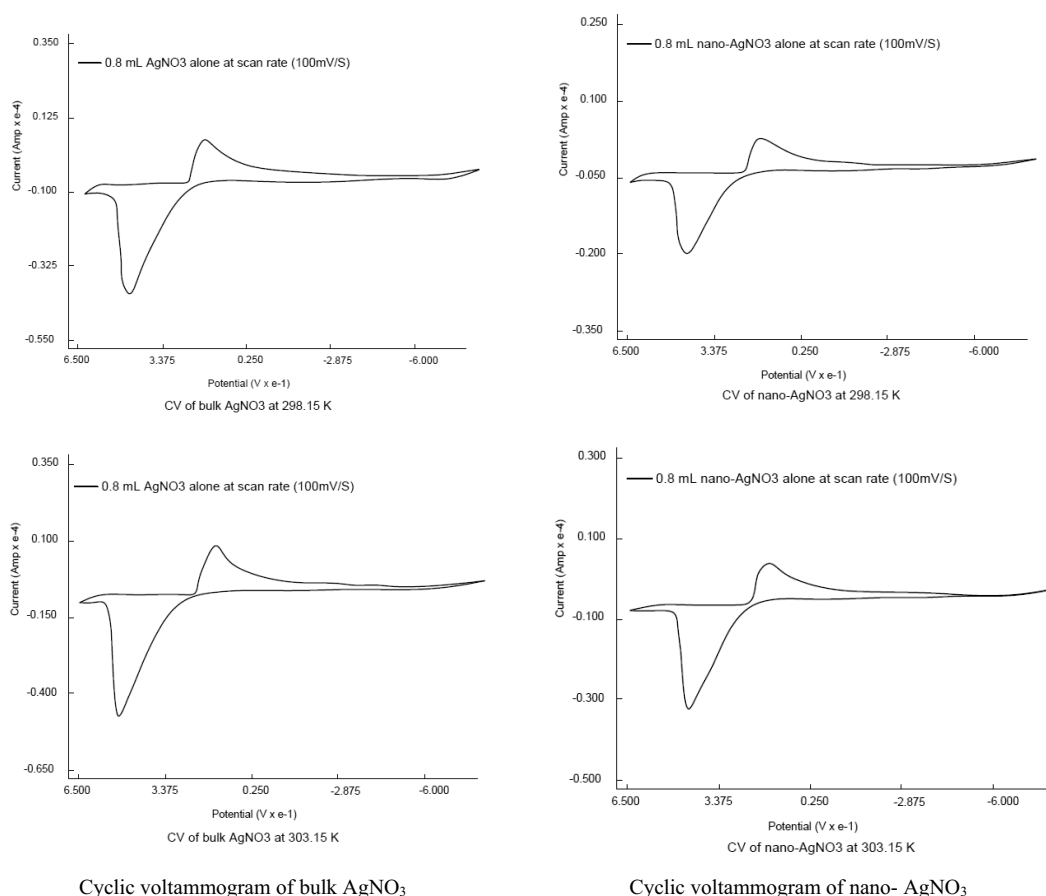


Fig. 3. cyclic voltammograms of bulk AgNO₃ and nano- AgNO₃ (NSN) in 0.1M KNO₃ at 298.15, 303.15 K.

3. 3. Electrochemical Behavior of Bulk AgNO₃ and Nano-AgNO₃ (NSN) in the Presence of Ligand (Cefdinir Antibiotic)

In this paper, we are studying the complexation between cefdinir drug and AgNO₃ in bulk and nano-scale in 5% mixed solvent (DMF-H₂O) at different temperatures (298.15, 303.15 K). In which the drug is added in a stepwise manner. Fig. 4 represent the electrochemical behavior of complexation between silver ions in bulk and nano-scale and Cefdinir antibiotic (CFD) in 0.1 M KNO₃ in mixed solvent (DMF-H₂O) at (298.15, 303.15 K) at -600 mV to 650 mV potential windows, current 1mA and scan rate 100 mV/S.

From Fig. 4, it is observed that the complex is formed due to the anodic and cathodic peak decrease and potential shifts their position to

more lower values. Due to precipitating the complex during the process, no peak appeared. A stability constant is a measure of the strength of the interaction between the reagents that come together to form the complex. The stability constant (β_{MX}) for bulk AgNO₃ and nano silver nitrate (NSN) complexes in 0.1 M KNO₃ at -600 mV to 650 mV potential windows, current 1mA and scan rate 100 mV/S in mixed solvent (DMF-H₂O) at different temperatures (298.15, 303.15 K) for each additions are calculated [14] by applying Eq. (1).

$$(E_p)_M + (E_p)_C = 2.303 \frac{RT}{nF} \text{Log} \beta_{MX} + 2.303 \frac{RT}{nF} \text{Log} C_x \quad (1)$$

where (Ep)M is the peak potential of metal at

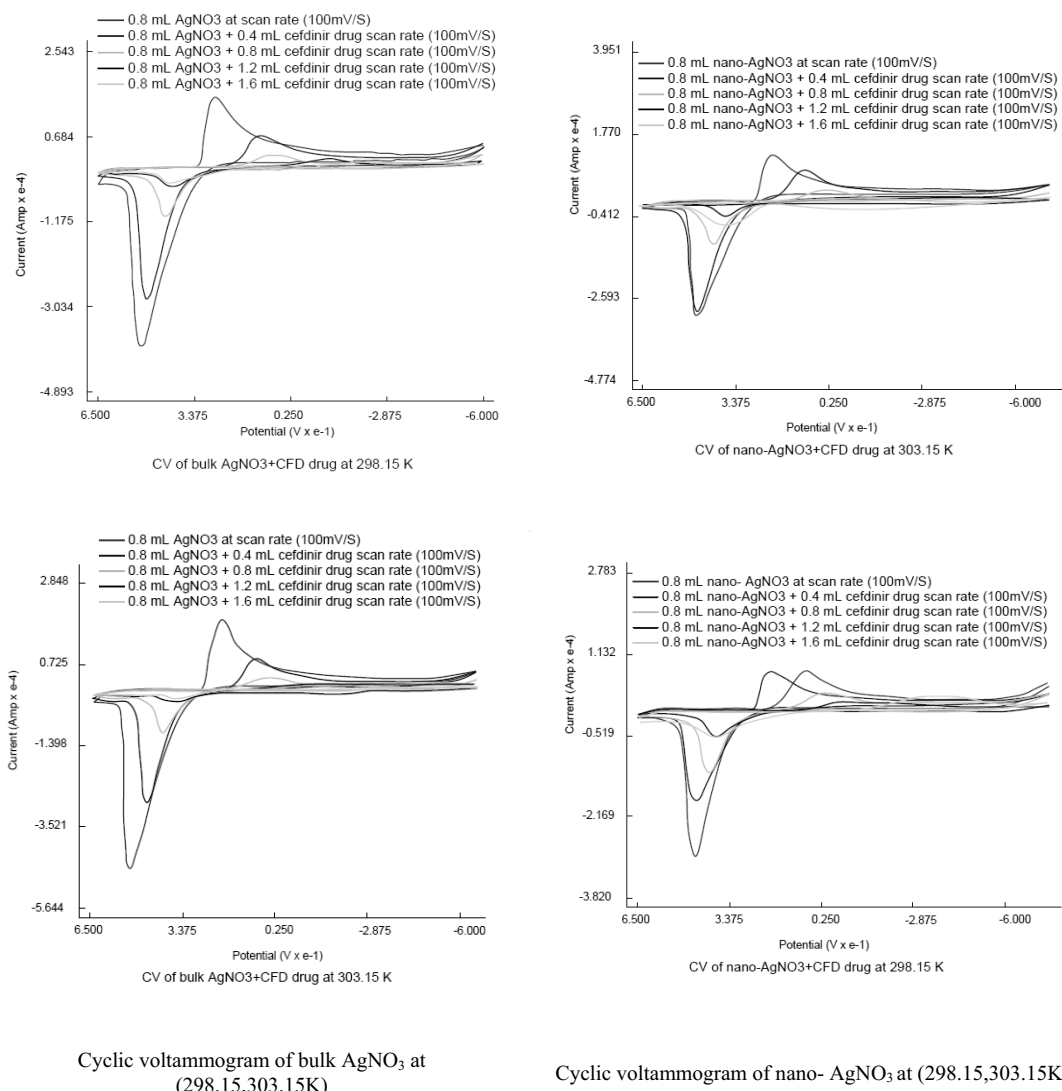


Fig. 4. Cyclic voltammograms of bulk AgNO₃ and Nano-AgNO₃ in the presence of cefdinir in 0.1 M KNO₃ at 298.15, 303.15 K.

final adding in absence of ligand, (Ep)C is the peak potential of metal complex, R is a gas constant (8.314 J.mol⁻¹.degree⁻¹), T is the absolute temperature and C_x is the concentration of metal in the presence of ligand.

The Gibbs free energy of interaction for bulk AgNO₃ and nano silver nitrate (NSN) with cefdinir antibiotic (CFD) were calculated [15,16] from stability constant (β_{MX}) using Eq (2).

$$\Delta G = -2.303 RT \log \beta_{MX} \quad (2)$$

All equilibrium constant vary with temperature, so the enthalpy (ΔH) of interaction for bulk AgNO₃ and nano-AgNO₃ (NSN) with cefdinir antibiotic (CFD) were calculated by using Van't Hoff Eq. (3). [17,18]

$$\log \frac{\beta_2(atT_2)}{\beta_1(atT_1)} = \frac{\Delta H}{2.303 R} \left(\frac{T_2 - T_1}{T_1 T_2} \right) \quad (3)$$

where β₁ is the stability constant at low temperature T₁, β₂ is the stability constant at high temperature T₂.

Table 1. Cyclic voltammetric data of bulk AgNO₃ and nano-AgNO₃ (NSN) in the presence of Cefdinir antibiotic at 298.15 K.

Bulk AgNO ₃ in the presence of Cefdinir in 5% mixed solvent (DMF-H ₂ O) at 298.15 K												
[M]X10 ⁻³	[L] X10 ⁻³	[M]/[L]	E _{p,a} /mV	E _{p,c} /mV	E _{1/2}	I _{p,a} /mA	I _{p,c} /mA	β	ΔG ^a	ΔH ^b	TAS ^c	ΔS ^d
1.89	0.474	4	558.9	136.8	347.85	-0.299	0.1261	3.37 x10 ⁴	-25.843	595.274	-621.117	-2.0832
1.87	0.936	2	492.7	128.5	310.6	-0.291	0.0768	1.29 x10 ⁶	-34.892	-12.139	-22.753	-0.0763
1.85	1.387	1.3	463.7	95.4	279.55	-0.179	0.0498	1.04 x10 ⁶	-34.361	-18.767	-15.594	-0.0523
1.82	1.827	1	430.6	74.7	252.65	-0.109	0.0325	8.20 x10 ⁵	-33.761	-2.975	-30.786	-0.1033
1.8	2.256	0.79	409.9	-49.5	180.2	-0.045	0.0227	1.98 x10 ⁴	-24.558	-6.998	-17.56	-0.0589
1.78	2.675	0.66	409.9	-107.5	151.2	-0.043	0.0206	1.99 x10 ⁴	-24.553	-13.415	-11.138	-0.0374
1.76	3.083	0.57	414.1	-198.5	107.8	-0.041	0.0185	2.06 x10 ⁴	-24.622	-29.749	5.127	0.0172
1.74	3.482	0.5	434.8	74.7	254.75	-0.035	0.0247	2.25 x10 ⁴	-24.850	-53.128	28.278	0.0948
Nano-AgNO ₃ in the presence of Cefdinir in 5% mixed solvent (DMF-H ₂ O) at 298.15 K												
[M]X10 ⁻³	[L] X10 ⁻³	[M]/[L]	E _{p,a} /mV	E _{p,c} /mV	E _{1/2}	I _{p,a} /mA	I _{p,c} /mA	β	ΔG ^a	ΔH ^b	TAS ^c	ΔS ^d
1.89	0.474	4	514	160	337	-0.3062	0.109	1.17 x10 ⁶	-34.641	8.728	-43.369	-0.1454
1.87	0.936	2	478	142	310	-0.2585	0.0756	8.91 x10 ⁵	-33.967	-1.010	-32.957	-0.1105
1.85	1.387	1.3	452	121	286.5	-0.1595	0.0473	7.36 x10 ⁵	-33.493	-8.612	-24.881	-0.0835
1.82	1.827	1	434	80	257	-0.1165	0.0287	6.39 x10 ⁵	-33.145	-4.051	-29.094	-0.0976
1.8	2.256	0.79	418	79	248.5	-0.0441	0.0158	5.81 x10 ⁵	-32.905	-536.086	503.181	1.6877
1.78	2.675	0.66	415	-8	203.5	-0.0434	0.0127	1.79 x10 ⁴	-24.285	-22.605	-1.68	-0.00563
1.76	3.083	0.57	407	-116	145.5	-0.0229	0.0098	1.76 x10 ⁴	-24.234	-26.040	1.806	0.00606
1.74	3.482	0.5	412	-240	86	-0.0245	0.0179	1.82 x10 ⁴	-24.313	-38.362	14.049	0.0471

Table 2. cyclic voltammetric data of bulk AgNO₃ and Nano-AgNO₃ in the presence of Cefdinir antibiotic at 303.15 K.

Bulk AgNO ₃ in the presence of cefdinir in 5% mixed solvent (DMF-H ₂ O) at 303.15 K												
[M]X 10 ⁻³	[L] X10 ⁻³	[M]/[L]	E _{p,a} /mV	E _{p,c} /mV	E _{1/2}	I _{p,a} /mA	I _{p,c} /mA	β	ΔG ^a	ΔH ^b	TAS ^c	ΔS ^d
1.89	0.474	4	528.9	142.8	335.85	-0.435	0.1509	1.77 x10 ⁶	-36.260	595.274	-631.53	-2.0832
1.87	0.936	2	476.6	119.9	298.25	-0.287	0.0915	1.19 x10 ⁶	-35.279	-12.139	-23.14	-0.0763
1.85	1.387	1.3	440.6	116.6	278.6	-0.167	0.0611	9.18 x10 ⁵	-34.612	-18.767	-15.84	-0.0523
1.82	1.827	1	420.9	77.4	249.15	-0.106	0.037	8.04 x10 ⁵	-34.275	-2.975	-31.3	-0.1032
1.8	2.256	0.79	391.5	-27.4	182.05	-0.034	0.0188	1.89 x10 ⁴	-24.827	-6.998	-17.83	-0.0588
1.78	2.675	0.66	378.4	-79.7	149.35	-0.025	0.0165	1.82 x10 ⁴	-24.727	-13.415	-11.31	-0.0373
1.76	3.083	0.57	355.5	-115.7	119.9	-0.018	0.0143	1.69 x10 ⁴	-24.535	-29.749	5.21	0.0172
1.74	3.482	0.5	335.9	-197.5	69.2	-0.016	0.121	1.58 x10 ⁴	-24.373	-53.128	28.76	0.0949
Nano-AgNO ₃ in the presence of Cefdinir in 5% mixed solvent (DMF-H ₂ O) at 303.15 K												
[M]X 10 ⁻³	[L] X10 ⁻³	[M]/[L]	E _{p,a} /mV	E _{p,c} /mV	E _{1/2}	I _{p,a} /mA	I _{p,c} /mA	β	ΔG ^a	ΔH ^b	TAS ^c	ΔS ^d
1.89	0.474	4	530	174	352	-0.433	0.1377	1.24 x10 ⁶	-35.361	8.728	-44.089	-0.1454
1.87	0.936	2	484.4	157.5	320.95	-0.287	0.0841	8.85 x10 ⁵	-34.519	-1.010	-33.509	-0.1105
1.85	1.387	1.3	451.3	140.9	296.1	-0.17	0.0521	6.95 x10 ⁵	-33.909	-8.612	-25.297	-0.0834
1.82	1.827	1	434.8	78.8	256.8	-0.111	0.0273	6.22 x10 ⁵	-33.631	-4.051	-29.58	-0.0976
1.8	2.256	0.79	401.7	4.3	203	-0.037	0.0165	1.64 x10 ⁴	-24.472	-536.086	511.61	1.6877
1.78	2.675	0.66	381	-41.2	169.9	-0.024	0.0144	1.54 x10 ⁴	-24.303	-22.605	-1.698	-0.0056
1.76	3.083	0.57	368.5	-169.5	99.5	-0.018	0.0165	1.48 x10 ⁴	-24.210	-26.040	1.83	0.00604
1.74	3.482	0.5	352	-173.7	89.15	-0.014	0.0144	1.41 x10 ⁴	-24.083	-38.362	14.279	0.0471

The entropy (ΔS) for bulk AgNO₃ and nano-AgNO₃ (NSN) complexes in 0.1 M KNO₃ at -600

mV to 650 mV potential windows, current 1mA and scan rate 100 mV/S in mixed solvent (DMF-

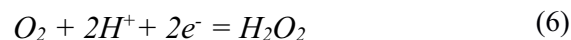
H₂O) at different temperatures (298.15, 303.15 K) are calculated by using Eq. (4) [19-30].

$$\Delta G = \Delta H - T\Delta S \quad (4)$$

The calculated values of (E1/2), (βMX), (ΔG), (ΔH), and (ΔS) for bulk AgNO₃ and nano-AgNO₃ (NSN) complexes in 0.1 M KNO₃ at -600 mV to 650 mV potential windows, current 1mA and scan rate 100 mV/S in mixed solvent (DMF-H₂O) at different temperatures (298.15, 303.15 K) are estimated in Tables 1, 2.

3. 4. MECHANISM OF THE REDOX REACTIONS

The reduction of tracers of dissolved oxygen play an important role in providing electrons required for silver dissolution process [19]. Eq. (5, 6) are represented silver dissolution.



From Fig. 3. Its observed that the main peak is the oxidation of silver (0) valent to silver (I) valent in 5% (DMF-H₂O) versus Ag/Ag+ electrode as shown by Eq. (5, 7). Hence, when adding cefdinir antibiotic to the composition caused decrease in both anodic and cathodic peak height respectively, which indicates the interaction between silver ions and cefdinir drug.

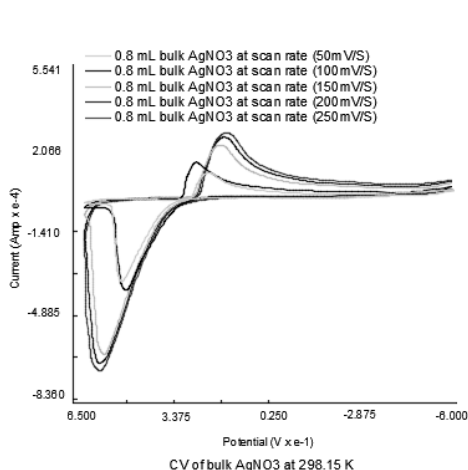


3. 5. VARIATION OF THE SCAN RATE

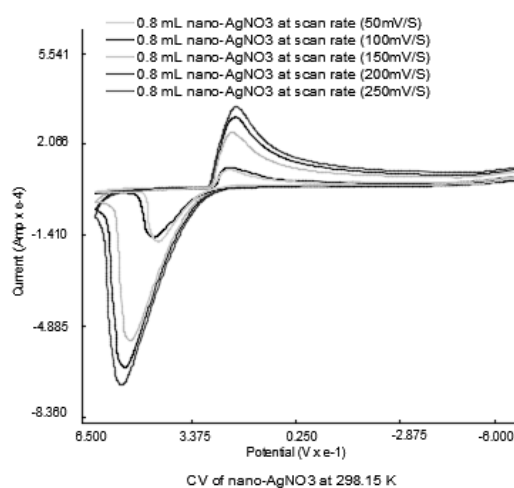
Cyclic voltammogram of bulk AgNO₃ and nano-AgNO₃ (NSN) in absence and presence of cefdinir

Table 3. cyclic voltammetric data of bulk AgNO₃ and nano-AgNO₃ (NSN) in absence of Cefdinir antibiotic in 0.1 M of KNO₃ at 298.15 K and different scan rates (50, 100, 150, 200 and 250 mV/S).

[M] x10 ⁻³	V/mV.S ⁻¹	V ^{1/2}	Bulk AgNO ₃				Nano-AgNO ₃			
			<i>I_{p,a}</i> /mA	<i>I_{p,c}</i> /mA	<i>D_a</i> /cm ² .s ⁻¹	<i>D_c</i> /cm ² .s ⁻¹	<i>I_{p,a}</i> /mA	<i>I_{p,c}</i> /mA	<i>D_a</i> /cm ² .s ⁻¹	<i>D_c</i> /cm ² .s ⁻¹
1.92	0.05	0.224	-0.357	0.154	1.16 x 10 ⁻¹⁰	2.16 x 10 ⁻¹¹	-0.198	0.0675	8.48 X 10 ⁻¹¹	9.86 X 10 ⁻¹²
1.92	0.1	0.316	-0.392	0.107	5.64 x 10 ⁻¹⁰	4.2 x 10 ⁻¹¹	-0.183	0.0768	3.64 X 10 ⁻¹¹	6.41 X 10 ⁻¹²
1.92	0.15	0.387	-0.669	0.239	1.09 x 10 ⁻⁹	1.39 x 10 ⁻¹⁰	-0.566	0.2163	7.84 X 10 ⁻¹⁰	1.14 X 10 ⁻¹⁰
1.92	0.2	0.447	-0.705	0.276	7.28 x 10 ⁻⁹	1.12 x 10 ⁻⁹	-0.669	0.2759	8.21 X 10 ⁻¹⁰	1.39 X 10 ⁻¹⁰
1.92	0.25	0.5	-0.739	0.297	6.39 X 10 ⁻⁹	1.03 X 10 ⁻⁹	-0.734	0.3125	7.89 X 10 ⁻¹⁰	1.43 X 10 ⁻¹⁰



Cyclic voltammogram of bulk AgNO₃



Cyclic voltammogram of Nano-AgNO₃

Fig. 5. Cyclic voltammogram of bulk AgNO₃ and Nano-AgNO₃ in absence of cefdinir antibiotic in 0.1 M of KNO₃ at 298.15 K and different scan rates (50, 100, 150, 200 and 250 mV/S).

Table 4. Cyclic voltammetric data of bulk and Nano-AgNO₃ in the presence of cefdinir antibiotic (1:1) and (1:2) in 0.1 M of KNO₃ at 298.15 K and different scan rates (50, 100, 150, 200 and 250 mV/S).

Bulk AgNO ₃ at (298.15 K)			(1:1)				(1:2)				
[M] x10 ⁻³	V/mV.S ⁻¹	V ^{1/2}	I _{p,a} /mA	I _{p,c} /mA	D _a /cm ² .s ⁻¹	D _c /cm ² .s ⁻¹	[M] x10 ⁻³	I _{p,a} /mA	I _{p,c} /mA	D _a /cm ² .s ⁻¹	D _c /cm ² .s ⁻¹
1.82	0.05	0.224	-0.055	0.0191	2.46 x 10 ⁻¹¹	2.96 x 10 ⁻¹²	1.74	-0.02	0.0185	2.84 x 10 ⁻¹¹	2.44 x 10 ⁻¹¹
1.82	0.1	0.316	-0.106	0.0325	4.59 x 10 ⁻¹¹	4.31 x 10 ⁻¹²	1.74	-0.035	0.0247	4.38 x 10 ⁻¹¹	2.18 x 10 ⁻¹¹
1.82	0.15	0.387	-0.111	0.0351	2.68 x 10 ⁻¹⁰	2.68 x 10 ⁻¹¹	1.74	-0.055	0.0283	7.21 x 10 ⁻¹¹	1.91 x 10 ⁻¹¹
1.82	0.2	0.447	-0.101	0.0351	1.66 x 10 ⁻¹⁰	2.01 x 10 ⁻¹¹	1.74	-0.055	0.033	5.40 x 10 ⁻¹¹	1.94 x 10 ⁻¹¹
1.82	0.25	0.5	-0.104	0.0377	1.41 x 10 ⁻¹⁰	1.85 x 10 ⁻¹¹	1.74	-0.055	0.04	4.32 x 10 ⁻¹¹	2.28 x 10 ⁻¹¹
NanoAgNO ₃ at (298.15 K)			(1:1)				(1:2)				
[M] x10 ⁻³	V/mV.S ⁻¹	V ^{1/2}	I _{p,a} /mA	I _{p,c} /mA	D _a /cm ² .s ⁻¹	D _c /cm ² .s ⁻¹	[M] x10 ⁻³	I _{p,a} /mA	I _{p,c} /mA	D _a /cm ² .s ⁻¹	D _c /cm ² .s ⁻¹
1.82	0.05	0.224	-0.0606	0.0237	2.98 x 10 ⁻¹¹	4.56 x 10 ⁻¹²	1.74	-0.0177	0.0206	2.23 x 10 ⁻¹¹	3.02 x 10 ⁻¹¹
1.82	0.1	0.316	-0.1165	0.0351	5.54 x 10 ⁻¹¹	5.03 x 10 ⁻¹²	1.74	-0.0188	0.0227	1.26 x 10 ⁻¹¹	1.84 x 10 ⁻¹¹
1.82	0.15	0.387	-0.119	0.0377	3.86 x 10 ⁻¹¹	3.86 x 10 ⁻¹²	1.74	-0.0352	0.0283	2.95 x 10 ⁻¹¹	1.91 x 10 ⁻¹¹
1.82	0.2	0.447	-0.114	0.0402	2.65 x 10 ⁻¹¹	3.29 x 10 ⁻¹²	1.74	-0.047	0.0309	3.94 x 10 ⁻¹¹	1.71 x 10 ⁻¹¹
1.82	0.25	0.5	-0.117	0.0428	2.23 x 10 ⁻¹¹	2.99 x 10 ⁻¹²	1.74	-0.05	0.033	3.57 x 10 ⁻¹¹	1.55 x 10 ⁻¹¹

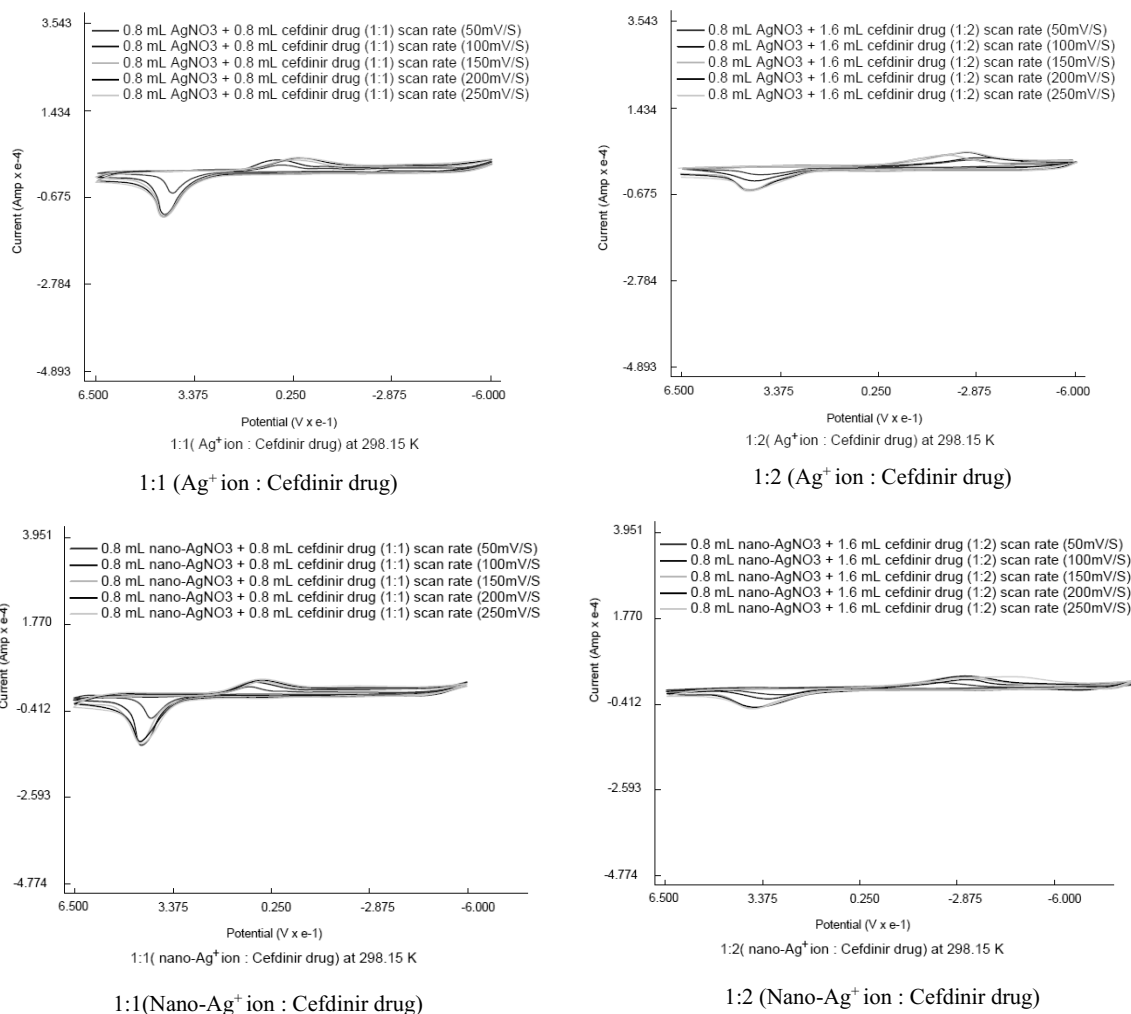
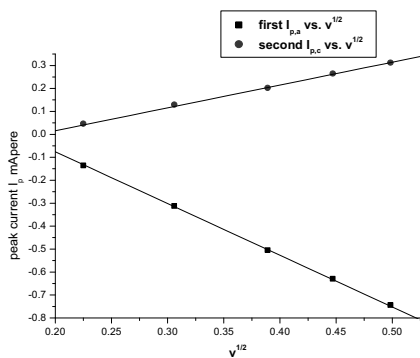
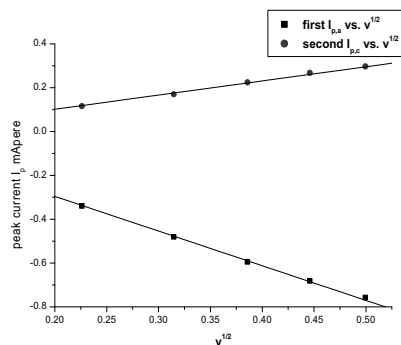


Fig. 6. Cyclic voltammogram of bulk and Nano-AgNO₃ in the presence of cefdinir antibiotic (1:1) and (1:2) in 0.1 M of KNO₃ at 298.15 K and different scan rates (50, 100, 150, 200 and 250 mV/S).

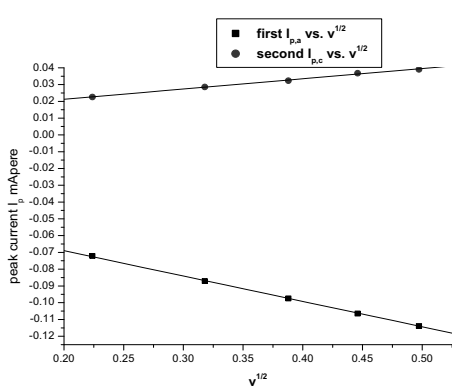


Peak current I_p vs. $V^{1/2}$ for bulk $AgNO_3$

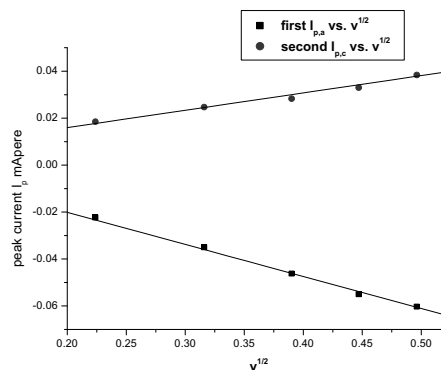


Peak current I_p vs. $V^{1/2}$ for Nano- $AgNO_3$

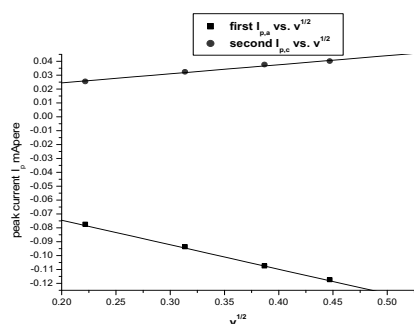
Fig. 7. The plot of both anodic and cathodic peak current against the scan rates at 298.15 K for bulk $AgNO_3$ and nano- $AgNO_3$ (NSN) in absence of Cefdinir antibiotic.



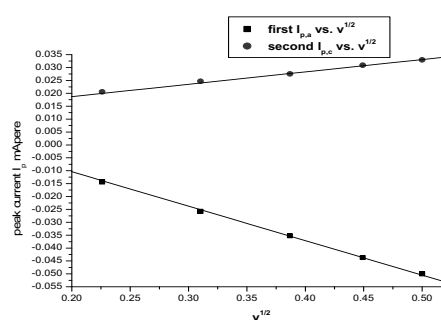
Peak current I_p vs. $V^{1/2}$ for bulk $AgNO_3$ (1:1)



Peak current I_p vs. $V^{1/2}$ for bulk $AgNO_3$ (1:2)



Peak current I_p vs. $V^{1/2}$ for nano- $AgNO_3$ (1:1)



Peak current I_p vs. $V^{1/2}$ for nano- $AgNO_3$ (1:2)

Fig. 8. The plot of both anodic and cathodic peak current against the scan rates at 298.15 K for bulk and nano- $AgNO_3$ (NSN) in the presence of Cefdinir antibiotic.

antibiotic in 0.1 M of KNO_3 at -600 mV to 650 mV potential windows, current 1mA and different scan rates (50, 100, 150, 200 and 250 mV/S) at absolute temperature 298.15 K. Represented in Figs. 5, 6. The peak current [20] for both the anodic and cathodic peaks follows Eq. (8).

$$I_p = 2.69 \times 10^5 n^{3/2} AC \sqrt{DV} \quad (8)$$

I_p =peak current in ampere, n =number of exchanged electrons, A =area of the in mol/cm^3 , V =scan rate in volts/S. electrode in cm^2 , D =diffusion coefficient in cm^2/s , C =concentration of the species.

The plot of both anodic and cathodic peak current against the scan rates (50, 100, 150, 200 and 250 mV/S) at 298.15 K for bulk AgNO_3 and nano silver nitrate (NSN) in absence and presence of cefdinir antibiotic in 0.1 M of KNO_3 at -600 mV to 650 mV potentials, current 1mA are shown in Figs. 7, 8 and the resulting data are listed in Tables 3, 4 .

From Fig. 6. It is observed that the scan rate of the complex mixtures increases the corresponding current increases and the slopes are in 0.5 range, so The electrochemical processes are diffusion controlled which confirmed from the graph of i_p vs $v^{1/2}$ as shown in the figures 7, 8. Also It was observed that the stability constants and the different thermodynamic properties are greater for the interaction of nano silver nitrate with Cefdinir drug at 298.15K whereas the bulk gave greater interaction values at the higher temperature due the fast migration of nano particles in complex area.

4. CONCLUSION

From Cyclic voltammetry (CV) data for bulk and nano AgNO_3 (NSN) in absence and presence of Cefdinir antibiotic we observe Ag^+ is electroactive giving one anodic and one cathodic peaks. Whereas in presence of Cefdinir (CEF) the anodic and cathodic peaks decrease in current and the potential shifts to more lower values due to the formation of complex. From stability constants and thermodynamic parameters for (1:1) stiochiometric metal to ligand ratio and (1:2) at the temperatures used. The enthalpies and entropies values are negative one for (1:1) while enthalpies values for (1:2) are negative and the entropies are positive.

From the effect of scan rates we indicate the redox process is diffusion controlled.

REFERENCES

1. Heilmann, A., Werner, J., Schwarzenberg, D., Henkel, S., Grosse, P. and Theib, W., "Microstructure and optical properties of plasmopolymer thin films with embedded silver nanoparticles", *Thin Solid Films*, 1995, 270, 103-108.
2. Giersig, M. and Mulvaney, P., "Preparation of ordered colloid monolayers by electrophoretic deposition", *Langmuir*, 1997, 9 (12), 3408-3413.
3. Sibbaldm, M. S., Chumanov, G., Cotton, T. M., "Reductive properties of iodide-modified silver nanoparticles", *J. Electroanal. Chem*, 1997, 438, 179-185.
4. Fajerwerg, V., Ynam, B., Chaudret, V., Garcon, D., Thouron, M. and Comtat, M., "An original nitrate sensor based on silver nanoparticles electrodeposited on a gold electrode", *Electrochem. Commun*, 2010, 12, 1439-1441.
5. Dhanya, S., Saumya, V. and Rao, T. P., "Synthesis of silver nanoclusters, characterization and application to trace level sensing of nitrate in aqueous media", *Electrochim. Acta*, 2013, 102, 299-305.
6. Kalfagiannis, N., Karagiannidis, P. G., Pitsalidis, C., Panagiotopoulos, N. T. and Logothetidis, S., "Performance of hybrid buffer Poly(3,4-ethylenedioxythiophene) poly (styrenesulfonate) layers doped with plasmonic silver nanoparticles", *Thin Solid Films*, 2014, 27-33, 104, 165.
7. Guo, L., NIE, J., DU, B., Peng, Z., Tesche, B. and Kleinermanns, K., "Thermoresponsive polymer-stabilized silver nanoparticles", *J. Colloid Interface Sci*, 2008, 319, 175- 181.
8. Lansdown, A. B. G., "Silver Pharmacological and Toxicological Profile as Antimicrobial Agent in Medical Devices", *Crit. Rev. Toxicol*, 2007, 37, 237-250.
9. Naodovic, M. and Yamamoto, H., "Asymmetric Silver-Catalyzed Reactions", *Chem*. 2008, Rev 108, 3132-3148.
10. Ito, Y., Sawamura, M. and Hayashi. T., "Gold- and Rhodium-Catalysed Aldol Additions", *J. Am. Chem. Soc* 1986, 108, 6405-6406.
11. Hamada, M. A., E. A., Gomaa, E. A. and El-Shishtawi, N. A., "Optomechanical properties of

- 10% PVA in presence of CoCl_2 and 44% ethanol water compositions, *International Journal of Optoelectronic engineering*, 2012, 2(1)1-3.
12. Gomaa, E. A. and Al Jahdali, B. A., "Conductometric studies of ionic association of divalent electrolyte $\text{Cu}(\text{NO}_3)_2$ with Kryptofix-22 in mixed MeOH-DMF solutions at different temperatures, *American Journal of Condensed Matter Physics*, 2012, 2(1)16-21.
 13. Gomaa, E. A., Galal, R., "Molar solubility, solvation and conductivity association parameters of sodium fluoride in mixed aqueous-ethanol solvents at different temperatures", *Basic Sciences of Medicine*, 2012, 1(2), 1-5.
 14. Ibrahim, K. M., Gomaa, E. A., Zaky, R. R., Abdel El-H. and Mahmoud, N., "The association and formation constants for CuCl_2 stoichiometric complexes with (E)-3-oxo-N-(thiazol-2-yl)propanamide in absolute ethanol solution", *American Journal of Chemistry*, 2012, 23-26.
 15. El-Khouly, A. A., Gomaa, E. A. and Salem, S. E., "Conductometric study of complex formation between 2, 3-pyrazine di-carboxylic acid and some transition metal ions in methanol", *Southern Brazilian Journal of Chemistry*, vol.20, no., 2012, 20, 43-50.
 16. Gomaa, E. A. and Al-Jahdali, B. M., "Electrical conductance of $\text{Cu}(\text{NO}_3)_2$ with Kryptofix-222 in mixed (MeOH-DMF) solvents at different temperatures", *American Journal of Environmental Engineering*, 2012, 2(2), 6-12.
 17. Gomaa Esam, A., "Molar solubility, dissociation and solvation parameters for saturated benzoic acid solutions in various solvents at 298.15 K., Esam A. Gomaa", *Physics and Chemistry of Liquids*, 2012, 50, 279-283.
 18. Gomaa, Esam, A., "Solubility and solvation parameters of barium sulphate in mixed ethanol-water mixtures at 301.15K, , *International Journal of Materials and Chemistry*, 2012, 2(1), 16-18.
 19. Gomaa, E. A., "The microscopic free energies of solvation for K^+ , Rb^+ and Cs^+ in mixed methanol (MeOH)-dimethyl formamide (DMFA) solvents at 298.15K", *International Journal of Theoretical and Mathematical Physics*, 2(2), 2012, 1-4.
 20. Abd El-Hady, Zaky, R. R., Ibrahim, K. M. and Gomaa, E. A., "(E)-3-(2-(furan-2-ylmethylene)hydrazinyl)-3-oxo-N-(thiazol-2-yl) propanamide complexes: synthesis, characterization and antimicrobial studies, *Journal of Molecular Structure*, 2012, 1016, 169-180.
 21. Gomaa, E. A., "Solubility and solvation parameters of calcium carbonate in mixed ethanol-water mixtures at 301.15K, *Science and Technology*, 2012, 2(1), 51-52.
 22. Kashyout, A. B., Soliman, H. M., Fathy Marwa, Gomaa, E. A. and Zidan, A., "CdSe Quantum dots for solar cell devices", *International Journal of Photoenergy*, 2012, 1-7.
 23. Gomaa, E. A. and Al Jahdali, B. A. M., "Electrochemical studies of cadmium ion with Kryptofix 22 in MeOH-DMF solutions at different temperatures", *Science and Technology*, 2012, vol.2, no.4, 1-8.
 24. Gomaa, E. A., "Gibbs free energies, enthalpies and entropies of transfer for reference ions Ph_4As^+ and Ph_4B^- in mixed DMFA-H₂O solvents at different temperatures", *American Journal of Environmental Engineering*, 2012, 2(3), 54-57.
 25. Gomaa, E. A., "Thermodynamic and polarization parameters of dibenzo-18-crown-6 in mixed methanol water solvents, *American Journal of Polymer Science*, 2012, 2(3), 35-38.
 26. Gomaa Esam, A. and Al Jahdali, B. A. M., "Conductometric studies of calcium ions with Kryptofix 221 in mixed MeOH-DMF solvents at different temperatures, *Education*, 2012, 2(3), 22.
 27. Hayashi, T., Vadim, E., Soloshonok, A. and Uozumi, Y., "Erythro-Selective aldol-type reaction of N-sulfonylaldimines with methyl isocyanacetate catalyzed by gold(I)", *Tetrahedron*, 1996, Lett. 28, 4969-4972.
 28. Jia, J., Hubberstey, P., Champness, N., Schröder, M., "Supramolecular Chemistry of 4, 4'-Bipyridine-N, N'-dioxide in Transition Metal Complexes: A Rich Diversity of Co-ordinate", *Hydrogen-Bond and Aromatic Stacking Interactions, Molecular Networks*, 2009, 135-161.
 29. Headridge, B. J., "Electrochemical Techniques for Inorganic Chemists Academic Press", London and New York, 1969.
 30. Berne, D. and Popovych, O., "Solubilities and medium effects of tetraphenylgermane, tetraphenylmethane, and tetraphenylsilane in acetonitrile, methanol, and some ethanol-water solvents, *Analytic. 1972, Chem. 44*, 817-820.